ELSEVIER

Materials Science and Engineering A293 (2000) 157–164

MATERIALS SCIENCE & ENGINEERING A

www.elsevier.com/locate/msea

High strain rate compression of closed-cell aluminium foams

Kathryn A. Dannemann *, James Lankford Jr.

Southwest Research Institute™, Mechanical and Materials Engineering Division, 6220 Culebra Road, San Antonio, TX 78238, USA

Received 24 March 2000; received in revised form 22 May 2000

Abstract

The compressive deformation behavior of open- and closed-cell aluminum foams was assessed under static and dynamic loading conditions. High strain rate experiments were conducted in our laboratory using a split Hopkinson pressure bar system at strain rates ranging from 400 to 2500 s^{-1}. A strain rate effect was demonstrated for Alporas, a closed-cell aluminum. foam. The strain-rate effect was more significant for a higher density (i.e. 15% relative density) Alporas foam and is attributed to the kinetics of gas flow through the cell structure. The experimental results are discussed in reference to recent findings by other investigators on the dynamic behavior of similar open- and closed-cell aluminum foams.

Keywords: Aluminum foam; Closed-cell; Open-cell; Compression; High strain rate

1. Introduction

Recent process developments have resulted in new and improved porous metallic materials. Although closed-cell aluminum foams are most commonly produced, other metal foams (e.g. titanium, nickel and steel) are becoming more commonplace as alternative processes and foaming agents are implemented. The relative densities of currently available foams range from 3% to 80%, though the lower density foams are more routine. Advances in near net shape processing of cellular metals have expanded the possible geometries. Thus, the feasibility of utilizing porous materials in structural applications is improving. A metal foams design guide [1] was recently published to aid in the implementation of these materials in various structural applications. Metal foams may provide a distinct advantage over solid metals for energy absorption applications.

The deformation behavior of metal foams has been investigated recently, though to a lesser extent than elastomeric foams. A comprehensive, general treatment, based on the relevant material properties, is provided by Gibson and Ashby [2]. Intrinsic strength is further accounted for in the work of Sugimara et al. [3] and others [4,5]. Recent investigations address the effects of defects on the quasistatic performance of metal foams. Simone and Gibson [6] found that face curvature and face corrugations can significantly reduce the modulus and peak stress of metal foams. These variables may account for some of the order of magnitude decreases in the mechanical properties of conventional, low relative density, metal foams versus those predicted by idealized models. Grenestedt [7] modeled the effects of 'imperfections', such as wavy distortions of cell walls, variations in cell wall thickness, non-uniform cell shape, etc., on the mechanical properties of cellular solids. This model suggests that structural stiffness is most sensitive to cell wall waviness with up to a 50% stiffness reduction for only moderately wavy imperfections. The relative insensitivity of stiffness in this model to even quite large cell wall thickness variations and cell shape variations is remarkable. These recent studies confirm the contribution of intrinsic cell structure to the mechanical performance of metal foams.

Strain rate effects are well documented for the dynamic loading performance of elastomeric foams [8–11]. Strength increases are observed with increasing strain rate for polymer foams, and are attributed to material properties as well as to viscous effects caused by fluid (i.e. gas) flow through pores. The effect of

* Corresponding author. Tel.: +1-210-5222523; fax: +1-210-5226290.

E-mail addresses: kdannemann@swri.org (K.A. Dannemann), jlankford@swri.org (J. Lankford Jr.).

0921-5093/00/$ - see front matter
PII: S0921-5093(00)01219-3

strain rate on the deformation behavior of porous metals has received consideration only recently. Limited work on strain rate effects in porous metals shows that the strain-rate sensitivity varies with the specific material, geometry and processing method. Mukai et al. [12] report the observance of a strain rate effect for Alporas, closed-cell aluminum foam (relative density = 0.10). The extent of the effect is illustrated in Fig. 1. In contrast, a closed-cell, Alulight foam, formed by a powder processing technique, did not exhibit a strain rate effect [13]. Tests in our laboratory on open-cell Al foam showed no dependence of compressive strength on loading rate [14], and this has been confirmed by Deshpande and Fleck [13]. A schematic illustrating the findings of Deshpande and Fleck [13] is shown in Fig. 2. Additional investigations have been conducted in our laboratory on open- and closed-cell (Alporas) metal foams in an effort to better understand the factors contributing to strain-rate dependency in these materials.

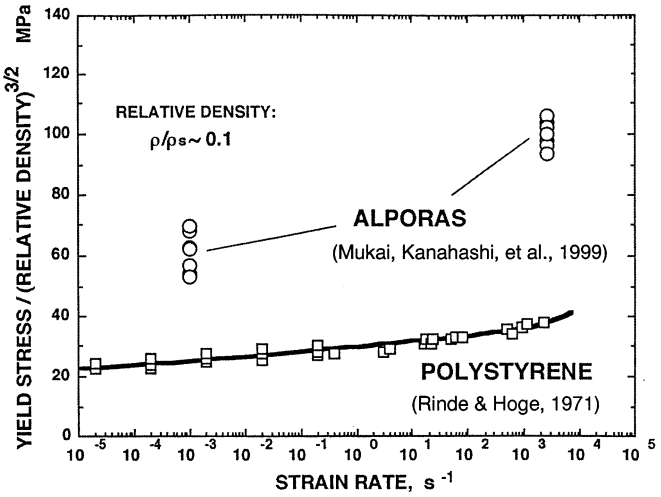

Fig. 1. The increase in normalized yield stress with increasing strain rate is indicative of a strain rate effect [from ref. 12].

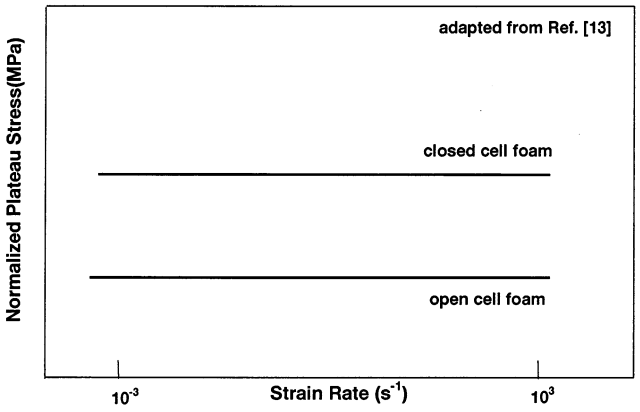

Fig. 2. A schematic created from the data of Deshpande and Fleck [ref. 13] showing the absence of a strain rate effect for closed-cell Alulight foam and open-cell Duocel foam.

2. Experimental

Closed-cell Alporas aluminum foam was provided by Shinko Wire (Amagasaki, Japan) for testing and evaluation. Alporas foams with approximate relative densities of 7.4 and 15% were investigated. The cell size of these foams is approximately 4–7 mm for the lower density foam, and 2–3 mm for the higher density foam. The closed cell microstructures are compared in Figs. 3(a) and (b). The cell aspect ratio differed for the Alporas foams investigated. Thus, the higher relative density foam contained more spheroidal cells versus a polyhedral shape for the lower density foam. Duocel™, open-cell aluminum foam, manufactured by Energy Research and Generation, Inc., was also evaluated. The 6101 aluminum, open-cell foam also had a relative density of 7%, and contained approximately 16 cells per cm (i.e. 40 pores per inch). The open-cell microstructure is shown in Fig. 3(c). Solid 6101 aluminum material of the same composition as the open-cell foam was tested for comparison with the open-cell foam.

Cylindrical test samples were electrodischarge machined from blocks of the Alporas and Duocel™ material. The Alporas samples measured 2.36 cm in diameter and 2.54 cm long. The open-cell foam and solid 6101 aluminum samples measured 0.95 cm in diameter and 1.90 cm long. The sample dimensions were chosen to allow a maximum number of cells across the diameter within the limitations of the available Hopkinson bar geometries. Since the open-cell foam averaged 16 cells per cm, there were sufficient cells across the 0.95 cm diameter to adequately represent the material behavior of the Duocel™ foam. The test sample size for the closed-cell foam is illustrated in the photos shown in Figs. 3(a) and (b). The photo height corresponds to the actual sample diameter, the photo width corresponds to the sample height. Thus, the number of cells across the sample diameter approached seven for the lower density Alporas foam, and exceeded seven for the higher density Alporas foam.

High strain-rate tests were conducted on the cylindrical samples described above using a split Hopkinson pressure bar apparatus. Dynamic compression tests were conducted at room temperature in laboratory air at strain rates ranging from 400 to 2500 s^{-1}. Aluminum transmitter and impactor bars were utilized; strain gages were installed on the pressure bars. For tests on the open-cell foam and solid 6101 aluminum samples, the pressure bars were approximately 1.25 cm in diameter. Further testing details are provided in ref. [14]. The diameter of the bars utilized for the closed-cell tests measured approximately 2.5 cm. A servo-controlled hydraulic test machine was used for low strain rate (10^{-4} to 10^{-3} s^{-1}) compression tests.

The open-cell foam and solid 6101 aluminum samples, as well as some of the Alporas samples, were fully compressed during dynamic compression tests. Interrupted, high strain rate compression tests were also conducted on the closed-cell Alporas foam to allow examination of deformed microstructures at a series of increasing strains. This was accomplished with the use of steel spacers to limit the maximum strain response. Alporas samples were evaluated prior to testing, and after high strain rate compression to approximately

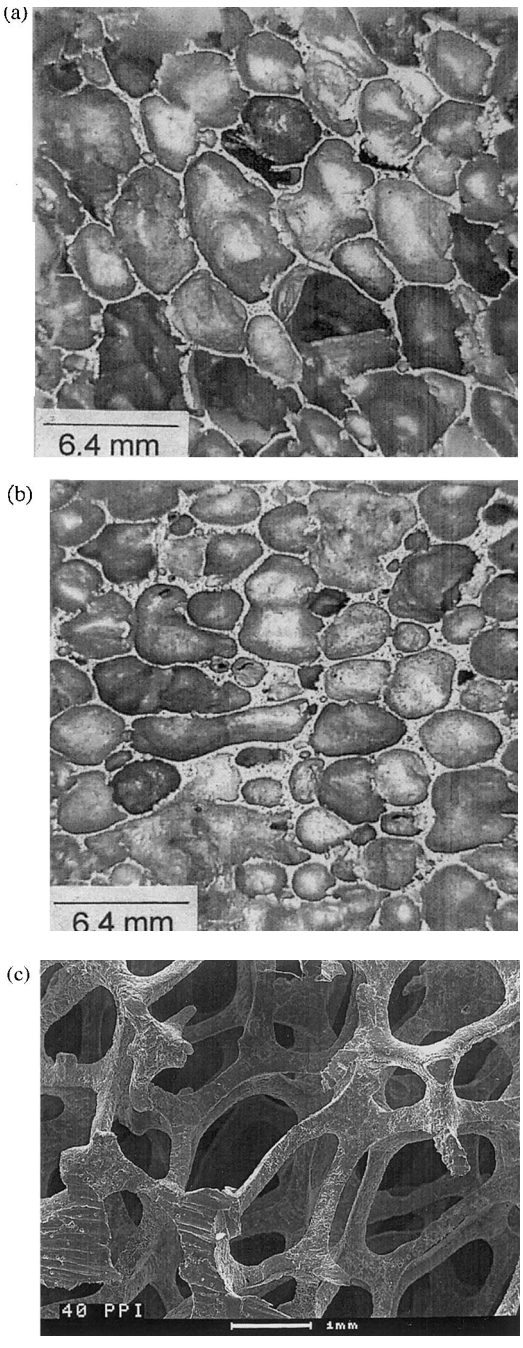

Fig. 3. Representative microstructures: (a) Closed-cell Alporas foam, $\rho/\rho_s = 0.07$; (b) closed-cell Alporas foam, $\rho/\rho_s = 0.15$; (c) open-cell Duocel foam, $\rho/\rho_s = 0.07$.

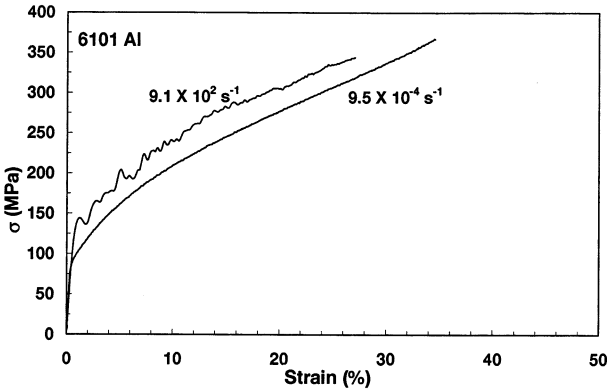

Fig. 4. Static and dynamic compressive stress-strain response of bulk 6101 aluminum. Each curve represents a single test.

3–4% and 9–10% strain. The 3–4% strain level was chosen since it represented a region on the stress-strain curve near the onset of the plateau region. The 9–10% strain level was more representative of the plateau region.

Compressed samples were evaluated with optical microscopy to determine the deformation modes. Following high strain rate testing, several Alporas samples were longitudinally sectioned by EDM for optical and scanning electron microscopy evaluation. The extent of cell wall deformation was investigated using the Southwest Research Institute (SwRI™) displacement mapping (DISMAP) system. This automated stereoimaging technique, developed at SwRI, measures material response by mapping the displacements within the material [15].

3. Results

A negligible strain-rate dependence was previously reported for the low density, open-cell aluminum foam tested in our laboratory [14]. Minimal energy absorption was observed, based on the stress-strain curves obtained. Compression tests on solid 6101 also revealed only a weak dependence of compressive strength on strain rate. These findings are compared in Figs. 4 and 5.

The results for the open-cell aluminum foam can be rationalized using the Gibson–Ashby [2] relationship for compressive strength controlled purely by plastic yielding within the cell walls.

$$\frac{\sigma^*_{pl}}{\sigma_y} = C(\rho/\rho_s)^{3/2}$$

where σ^*_{pl} is the critical compressive stress at collapse, and σ_y is the yield strength of the cell wall material. On this basis alone, there does not appear to be much chance for significant energy absorption enhancement due to higher loading rates. The yield strength of the

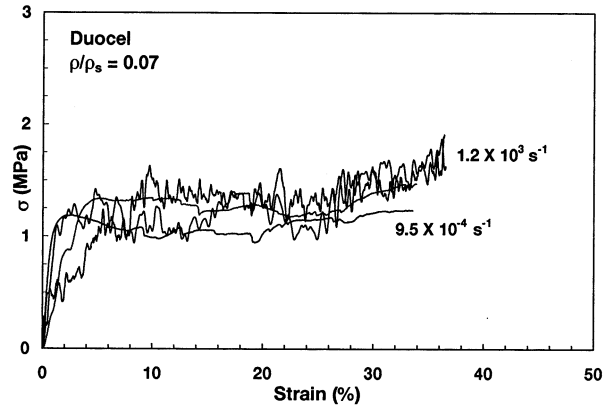

Fig. 5. Static and dynamic compressive stress-strain response of open-cell 6101 aluminum foam. Each curve represents a single test.

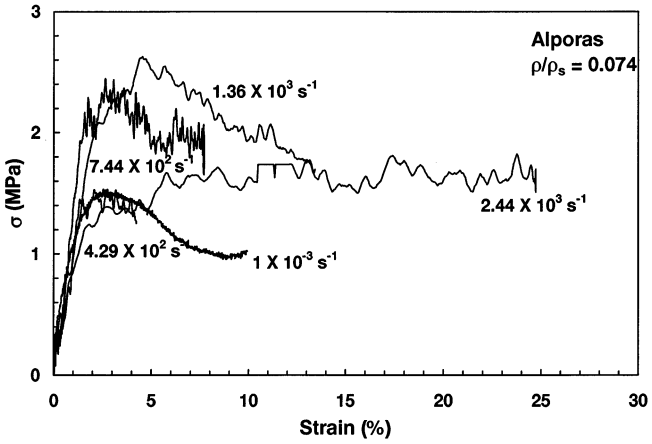

Fig. 6. Static and dynamic compressive stress-strain response of closed-cell Alporas foam ($\rho/\rho_s = 0.07$). Each curve represents a single test.

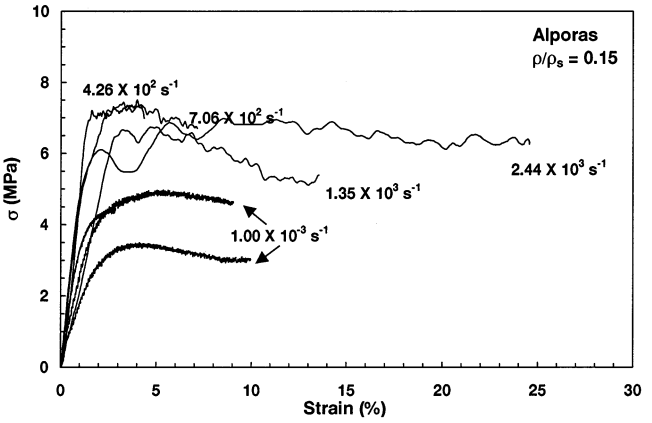

Fig. 7. Static and dynamic compressive stress-strain response of closed-cell Alporas foam ($\rho/\rho_s = 0.15$). Each curve represents a single test.

cell wall material, σ_y, is the only obvious strain rate dependent parameter in the equation, and as shown above, the yield strength dependence on strain rate for 6101 aluminum is weak.

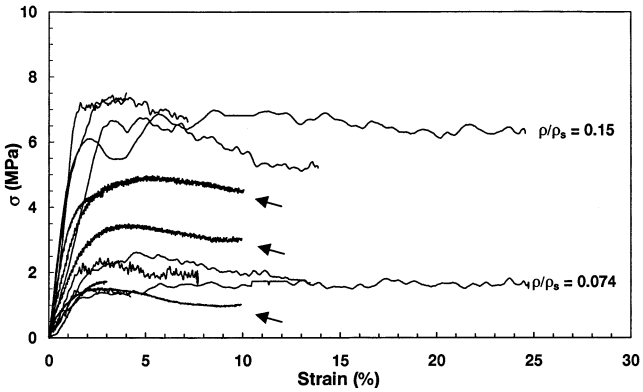

Fig. 8. Comparison plot of the data sets from Figs. 6 and 7 for closed-cell Alporas foam. The low strain rate data are identified by arrows. Two low strain rate curves are shown for the higher density ($\rho/\rho_s = 0.15$) foam.

In contrast, a strain-rate dependence was demonstrated for the closed-cell Alporas foam. The effect is shown in Fig. 6 for the lower relative density ($\rho/\rho_s = 0.07$) foam. An increase in maximum stress is evident for the higher strain rate tests relative to the quasistatic data. Each curve on the stress-strain plot represents a single test. The decline in stress at a strain rate of 2440 s^{-1} is likely an anomaly since an abundance of large open cells were detected around the periphery of this particular sample following optical microscopy inspection.

The strain-rate effect is more significant for the higher relative density ($\rho/\rho_s = 0.15$) foam, as shown in Fig. 7. Note the difference in the y-axis scaling for the plots in Figs. 6 and 7. Data comparison is simplified in Fig. 8 where the stress–strain results are cross-plotted on the same scale. The low strain-rate data are identified by arrows. The magnitude of the strain-rate effect is apparent.

Microstructural evaluation of samples following high strain-rate compression testing to different strain levels was beneficial in terms of understanding the nature of the deformation response. Representative SEM micrographs are shown in Figs. 9 and 10 for Alporas samples tested at 1100 s^{-1}. The micrographs in Fig. 9 are for the low relative density material; higher density closed-cell foam structures are shown in Fig. 10.

Slight deformation of the cell walls was evident at the lower strains (i.e. 3.3% and 4.7%; Fig. 9a and Fig. 10a) for the Alporas samples tested at approximately 1100 s^{-1}. These regions are highlighted by arrows in the figures. The overall extent of damage was low at low strain levels; few cell walls were ruptured. As expected, the extent of damage increased at higher strain levels (approaching 10%). Buckling of the cell walls occurred perpendicular to the compression axis at the higher

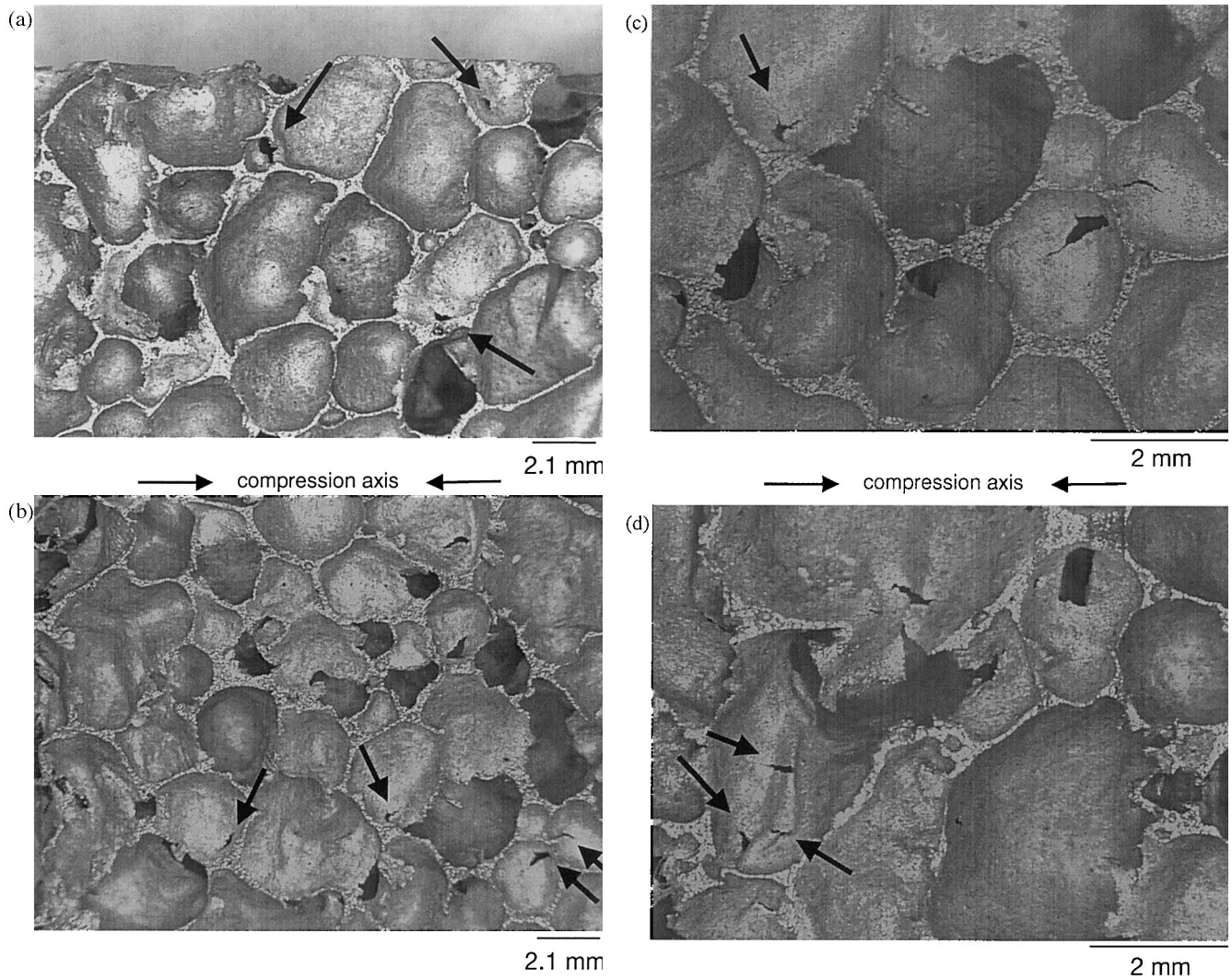

Fig. 9. Representative micrographs showing the progress of high strain-rate (1100 s^{-1}) compressive deformation in closed-cell Alporas foam with an approximate relative density of 7%. Fig. (c) is an enlargement of (b). (a) 3.3% strain; (b) 9.9% strain; (c) 9.9% strain; (d) 9.9% strain.

strain levels. Tearing of the walls is evident in some of the buckled regions; compare Figs. 9(c and d) and 10 (c and d). The majority of tears are oriented parallel to the compression axis. Some cell walls appear to have 'blown out' and ruptured. More cell wall damage also was evident at higher strains (approaching 10%) for the lower density Alporas foam.

4. Discussion

The results detailed above clearly show a strain rate effect for closed-cell Alporas foams. This is in agreement with the findings reported by Mukai et al. [12] for 10% dense Alporas foam. The differences depicted in the plot in Fig. 8 probably can be attributed to differences in cell shape, in agreement with the previous work of Bart-Smith et al. [4] and Miyoshi et al. [16]. High aspect ratio cell walls in the low relative density (7%) Alporas foam are associated with a polyhedral cell structure. For the higher density (15%) Alporas foam, the aspect ratio of the cell walls is lower and the cells are more spheroidal in shape. In the case of the slender aspect-ratio polyhedral cell walls, it is highly likely that 'wrinkles' formed in compressed walls early in the load history. These are intrinsically unstable, and can lead to independent, more-or-less simultaneous collapse of multiple walls. The cell walls associated with spheroidal cells are thicker on average, and the reduced length is too short to lead to compressive instability. In fact, these walls may experience some plastic deformation prior to cell wall rupture. This deformation mechanism is shown schematically in Fig. 11.

The extent of the observed strain rate dependence of Alporas is depicted in the normalized stress versus strain rate plot in Fig. 12. Data is included for Alporas,

including Mukai's [12] results, and for closed-cell Alulight [13]. Three factors that have been suggested as possible bases for such strain rate dependence include: (i) intrinsic material deformation; (ii) pressurization of the gas within the cells due to compression; and (iii) movement of the gas through the cells following cell wall rupture. However, the strain rate insensitivity of aluminum is well known and was further confirmed for 6101 aluminum in the present study. Pressurization of the gas (i.e. air) within the cells is also a strain-rate insensitive process. Thus, it follows that the movement of the gas through the cellular structure must be the major contributor to the observed phenomenon.

Inertia to the gas flow process results in a series of time dependent events. First, the buildup of pressure within the cell walls eventually causes some of them to rupture, a process that occurs in a series of isolated events. Specimen collapse occurs when there are no longer sufficient cell walls intact to support the compressive load. The maximum rate of damage propagation is limited by the speed of sound in the porous microstructure. Initial damage is likely concentrated at the sample surface, progressing with time through the sample and destabilizing sequentially the internal cell walls. Additional experiments are planned on the Alporas material to confirm this hypothesis.

It seems likely that the absence of a strain rate dependence in the Alulight material is related to the difference in processing technique. In particular, it is suspected that cell wall rupture may not necessarily

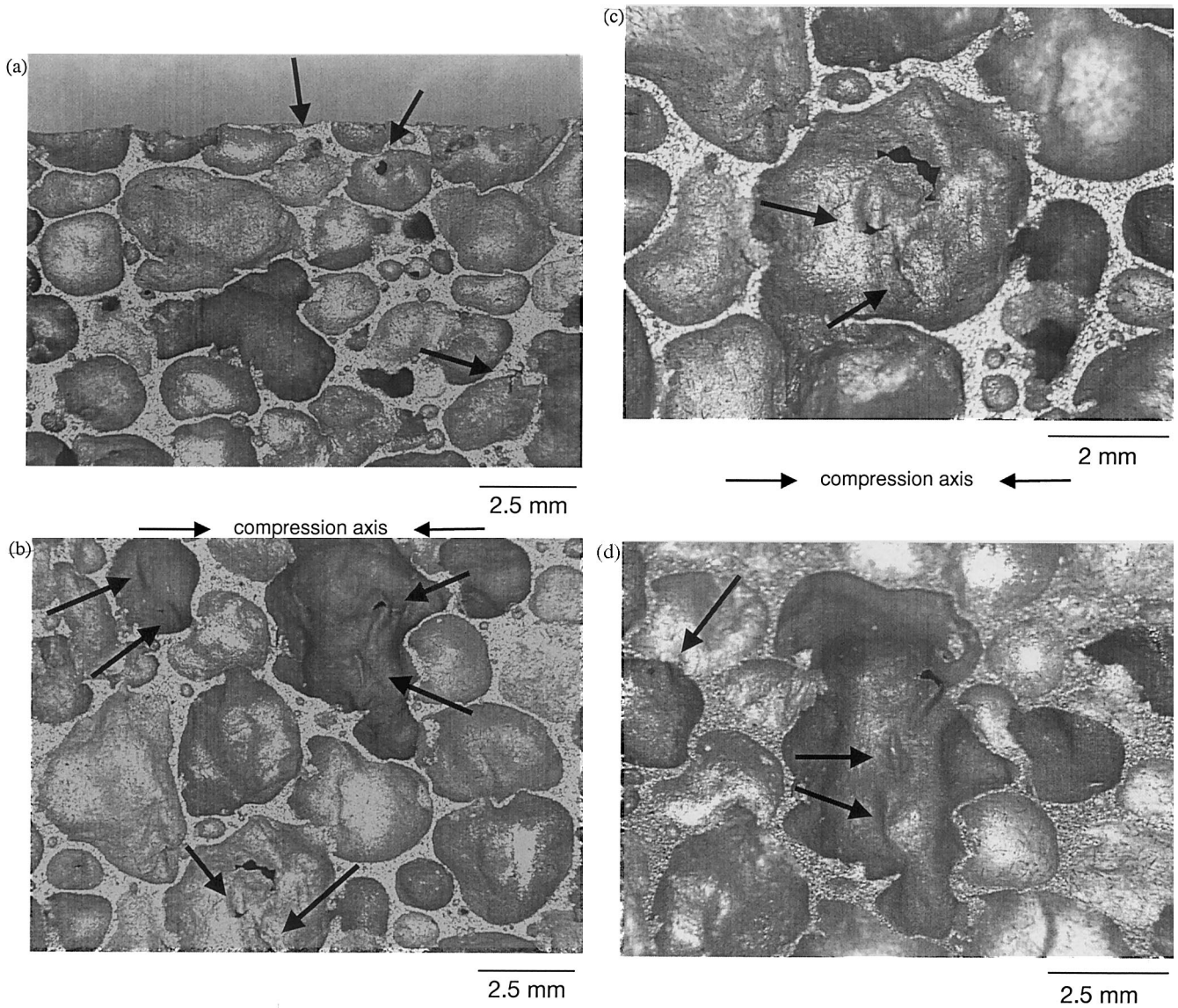

Fig. 10. Representative micrograph showing the progress of high strain-rate (1100 s^{-1}) compressive deformation in closed-cell Alporas foam with an approximate relative density of 15%. (c) and (d) are enlargements of (b). (a) 4.2% strain; (b) 10.7% strain; (c) 10.7% strain; (d) 10.7% strain.

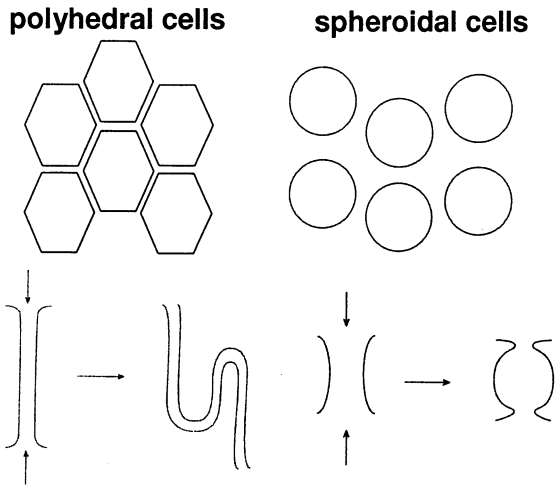

Fig. 11. Schematic depicting the effect of cell shape on the compressive deformation behavior of the Alporas foams. The lower drawings depict cell wall deformation for walls with different aspect ratio.

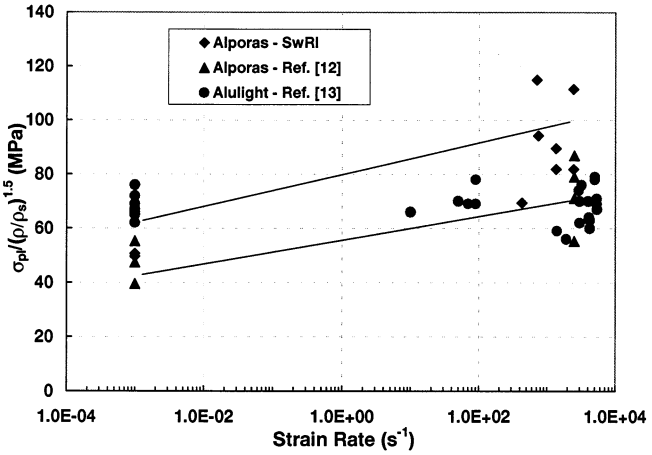

Fig. 12. Normalized stress versus strain rate plot for Alporas and Alulight foams showing a strain rate dependence for the Alporas foam.

occur as a series of isolated events. However, at this time it is not known precisely how the processing of Alulight manifests itself in a rnicrostructurally-controlled damage development sequence.

5. Conclusions

Investigations conducted in our laboratory indicate that strain rate strengthening occurs in closed-cell aluminum (Alporas) foams. The effect is more apparent for the higher density (15%) foam investigated. A strain rate effect also has been reported for 10% dense Alporas material in recent work by Mukai et al. [12]. Variance between these findings for Alporas and those of Deshpande and Fleck [13] for Alulight closed-cell metal foam are attributed to material/processing differences (casting vs. powder processing). The strain rate effect is thought to be related to fluid (air) flow through ruptured cell walls, and appears to be controlled by cell shape, cell size and distribution, cell wall aspect ratio and uniformity of wall section profile.

Acknowledgements

This work was supported by the Office of Naval Research, Contract N00014-98-C-0126, and was monitored by Dr Steven Fishman. The authors are grateful for the technical assistance of Arthur Nicholls in conducting the compression tests, and Byron Chapa and Isaac Rodriguez for characterizing the porous materials and test samples. The technical insights provided by Andrew Nagy are also gratefully acknowledged.

References

[1] M.F. Ashby, A.G. Evans, N.A. Fleck, et al., Metal Foams: A Design Guide, Butterworth Heinemann, Oxford, 2000.
[2] L.J. Gibson, M.F. Ashby, Cellular Solids: Structure and Properties, 2nd ed, Pergamon Press, Oxford, 1997.
[3] Y. Sugimura, J. Meyer, M.Y. He, H. Bart-Smith, et al., On the mechanical performance of closed cell Al alloy foams, Acta Mater. 45 (1997) 5245–5259.
[4] H. Bart-Smith, A.F. Bastawros, D.R. Mumm, et al., Compressive deformation and yielding mechanisms in cellular Al alloys determined using X-ray tomography and surface strain mapping, Acta Mater. 46 (1998) 3583–3592.
[5] J. Banhart, J. Baumeister, Deformation characteristics of metal foams, J. Mater. Sci. 33 (1998) 1–10.
[6] A.E. Simone, L.J. Gibson, The effects of cell face curvature and corrugations on the stiffness and strength of metallic foams, Acta Mater. 46 (1998) 3929–3935.
[7] J.L. Grenestedt, Influence of imperfections on effective properties of cellular solids, in: D.S. Schwartz, D.S. Shih, A.G. Evans, H.N.G. Wadley (Eds.), Porous and Cellular Materials for Structural Applications, Materials Research Society Symposium Proceedings, vol. 521, 1998, pp. 3–13.
[8] J. Zhang, M.F. Ashby, CPGS Thesis, Cambridge University Engineering Department, 1986.
[9] C.J. Tyler, M.F. Ashby, Project Report, Cambridge University Engineering Department, 1986.
[10] J.A. Rinde, K.G. Hoge, Time and temperature dependence of the mechanical properties of polystyrene bead foam, J. Appl. Polymer Sci. 15 (1971) 1377–1395.
[11] A. Nagy, W.L. Ko, U.S. Lindholm, Mechanical behavior of foamed materials under dynamic compression, J. Cellular Plastics 10 (1974) 1–8.
[12] T. Mukai, H. Kanahashi, T. Miyoshi, et al., Experimental study of energy absorption in closed-cell aluminum foam under dynamic loading, Scripta Met. 40 (1999) 921.
[13] V.S. Deshpande, N.A. Fleck, High strain rate compressive behavior of aluminum alloy foams, Int. J. Impact Eng. 24 (2000) 277–298.
[14] J. Lankford Jr., K.A. Dannemann, Strain rate effects in porous materials, in: D.S. Schwartz, D.S. Shih, A.G. Evans, H.N.G. Wadley (Eds.), Porous and Cellular Materials for Structural Applications, Materials Research Society Symposium Proceedings, vol. 521, 1998, pp. 103–108.

[15] D.L. Davidson, K.S. Chan, R.A. Page, Automated high-resolution displacement measurements for deformation and fracture research, in: W.N. Sharpe (Eds.), Micromechanics: Experimental Techniques (Book no. H00539), AMD-Vol. 102, 1989.
[16] T. Miyoshi, M. Itoh, S. Akiyama, A. Kitahara, Aluminum foam, Alporas: the production process, properties and applications, in: D.S Schwartz, D.S. Shih, A.G. Evans, H.N.G. Wadley (Eds.), Porous and Cellular Materials for Structural Applications, Ma terials Research Society Symposium Proceedings, vol. 521, 1998, pp. 133–137.